I. Dominguez, I. del Villar, J. Corres, J. Lachaud, Y. Yang, H. Hallil, C. Dejous and I. R. Matias, Analyst, 2022, 147, 5477 DOI: 10.1039/D2AN01371A

Spectral measurements with hybrid LMR and SAW platform for dual parameter sensing

Ismel Dominguez[1], Ignacio del Villar[1,2], Jesús Corres[1,2], Jean-Luc Lachaud[3], Yang Yang[3], Hamida Hallil[3], Corinne Dejous[3], Ignacio R. Matias[1,2]

[1] Electrical, Electronic and Communications Engineering Department, Public University of Navarra, 31006 Pamplona, Spain.

[2] Institute of Smart Cities (ISC), Public University of Navarra, 31006 Pamplona, Spain.

[3] Univ. Bordeaux, CNRS, Bordeaux INP, IMS, UMR 5218, F33400, Talence, France.

*email: jmcorres@unavarra.es

Abstract

Lossy mode resonance (LMR)-based optical sensors change their wavelength upon contact with substances or gases. This allows developing applications to detect the refractive index of the surrounding medium and even the thickness of the biolayers deposited on the waveguide. In the same way, when acoustic sensors are in contact with a liquid, it is possible to determine parameters, especially mechanical ones such as shape of the particle or molecule, mass load, elastic constants and viscosity of the liquid. This work reports the development of a system that combines LMR with surface acoustic wave (SAW) technologies to characterize a liquid in terms of its refractive index and viscosity simultaneously. Conveniently prepared glucose solutions are used for sensor calibration. The refractive index of the solutions ranges from 1.33 to 1.41 and its viscosity ranges from 1.005 mPa·s to 9 mPa·s, respectively. A sensitivity of 332 nm/RIU has been achieved with the optical sensor while the acoustic sensor has shown a sensitivity of -1.5dB/(mPa·s). This new combinational concept could be expanded to the development of more demanding applications such as chemical sensors or biosensors.

keywords: *multiparametric sensor platform, refractive index, viscosity, lossy-mode resonance, acoustic and optical transducers, chemical and biosensors.*

1. Introduction

In a world where new technology is constantly being developed and the amount of data, we receive daily is increasing, the unification and integration of systems that provide multiple parameter analysis is a growing trend. Multiparameter acquisition is a way to enrich our knowledge of the sample under test, and make it more accurate and reliable, by combining and comparing different data from the same source, in addition to saving a lot of time and resources. The sensor nodes used to monitor pollution in cities are an example of such sensor fusion, based on the integration of data and the consolidation of the information from the simultaneous acquisition of several variables.

Multiparameter approaches have been introduced in the world of emerging sensors. More than two decades ago, the different primary detection techniques: chemical, acoustic, optical, etc. began to converge and move towards new combined techniques. Infrared and visible spectroelectrochemistry, for example, as a multi-response analytical technique, provides unique insights into interfacial reaction and redox processes in the electrode[1]. Even using optical elements such as the microscope, it is possible to provide images that are complementary information for analysis. In another approach it is sometimes possible to enrich the signal of a single device, as proposed with surface acoustic wave devices, thus providing a multi-response with mechanical but also electrical sensitivity, that can be separated by using two readout frequencies or a time-gating technique[2].

Techniques such as surface plasmon resonance (SPR), lossy mode resonance (LMR) or Love waves surface acoustic waves (LW-SAW), among others, can be combined to obtain information related to both optical and mechanical parameters such as the refractive index and the viscosity of the fluids that come into contact with the sensor. There are several detailed reports in the last decade of successful attempts to combine optical and acoustic techniques such as SPR and LW-SAW. One of them aims at studying the adhesion of biomolecules on simple surfaces and focuses on the monitoring of the absorption of bovine serum albumin (BSA) on gold[3]. In it, a microfluidic cell made of PDMS is used to encapsulate the SAW surface and facilitate the confinement of the liquid. In another report, an instrument that combines the same techniques in real time, allows the identification of the water content in the protein layers of collagen and fibrinogen[4]. In addition, Bender *et al.* reports the development of a similar combined system for the investigation of biomolecules such as proteins or DNA [5]. In it, characterization by means of these techniques of the deposition of neutravidin and DNA is reported. All these publications demonstrate the above-mentioned advantages of combining complementary techniques for multiple parameters simultaneous sensing.

Regarding LW-SAW, they are of great interest as highly sensitive platform, especially adapted for liquid sensing. They are based on a principle that is similar to more conventional "SAW" devices, using Rayleigh waves, which have been extensively used for decades as delay-lines and mechanical filters for short-term precision clocks in a lot of applications such as telecommunications and sensors[6,7]. By comparison, LW-SAW devices are also fabricated using planar technologies, and the acoustic wave is also confined at the near surface. These features

allow for a good mechanical robustness and reproducibility thanks to the bulk substrate as mechanical support and collective production, and an outstanding sensitivity to surface mechanical changes thanks to the acoustic energy density profile. Furthermore, LW-SAW provide an additional advantage related to the shear horizontal wave polarization, which avoids too much energy coupling into an adjacent liquid, and as a result, allow for sensing applications in liquid media, whether for the rheological characterization of fluids or as biosensor[8].

Regarding LMRs, they are often confused with SPRs. Therefore, it is important to differentiate both phenomena. SPRs occur when the real part of the thin film's permittivity is negative and of greater magnitude than its own imaginary part and the permittivity of the material surrounding the thin film (i.e., the optical waveguide and the surrounding medium in contact). In contrast, LMRs occur when the real part of the permittivity of the thin film is positive and of greater magnitude than its own imaginary part and the material surrounding the thin film[9,10]. These different conditions explain why the kind of materials used to generate LMRs and SPRs is quite different. SPRs are typically obtained with metals while LMRs are obtained with metal oxides, said real part of the refractive index is high and the imaginary part is small [9].

This agrees well with the mode transition phenomenon, closely related to the lossy mode resonances (LMR) in the sense that a mode guided in the optical fiber experiences a transition to guidance in a thin-film with losses[11]. This results in a reduction of the transmitted power in a specific wavelength range, corresponding to the LMR generation by the guided mode coupled in the thin-film and that can be excited, contrary to SPRs, both for transversal electric (TE) and transversal magnetic (TM) polarized light [9]. In addition, as the thickness of the thin-film is increased, more LMRs can be generated, which leads to a multiresonance platform, that can be exploited for multiparameter sensing [12]. Moreover, the central wavelength of the LMR in the optical spectrum can be easily tuned by controlling the film thickness [13], thanks to the fact that many metallic oxides present a real part of their refractive index almost constant over a wide range of wavelengths. This is not possible with the materials that generate SPRs or LSPRs.

Regarding the sensitivity, it has been successfully proved that LMRs present better sensitivities than SPRs [14]. Moreover, using D-shaped fibers, it is possible to obtain sensitivities of more than 10^6 nm/RIU in the silica region (1.45 RIU) and of more than 10^4 nm/RIU in the water region (1.33 RIU)[15]. Since the sensitivity to refractive index (RI) is often used as a test for the prediction of the device performance, these values indicate the potential of this type of device for being used as a biosensor, with a couple of remarkable works: one where it was possible to detect immunoglobulin G at femtomolar concentration in human serum[16] and another one detecting D-dimer in human serum with a detection limit of 100 ng/mL, a value 5-fold below the clinical cutoff value of venous thromboembolism disease[17].

However, LMRs peaks are typically broader than SPRs, though again D-shaped fiber has been proved as the best structure for counteracting this limitation, because it permits to separate the TE and TM component of LMRs, which sometimes overlap each other in the optical spectrum[15]. Finally, it is important to mention that recently LMRs have been successfully

demonstrated in planar configuration, which simplifies the sensing system and also permits to separately extract the TE and the TM components[18,19]. Therefore, this configuration will be used in combination with acoustic sensor technology for detecting both viscosity and refractive index.

2. Methods and Materials

The proposed sensor, described in Figure 1, departs from a previously designed and tested LW-SAW sensor composed of a quartz crystal substrate with interdigitated electrodes and a SiO_2 waveguide layer. On top of the structure, a thin SnO_2 layer permits to generate the LMR with the aid of light transmitted and collected by multimode fibers (MMF). A visible polarizer makes it possible to separate the TE or TM component of light and improve the visualization of the LMR. A microfluidic structure ensures the confinement of the substances under study that will make contact with the surface. More details on each part are given in the next subsections.

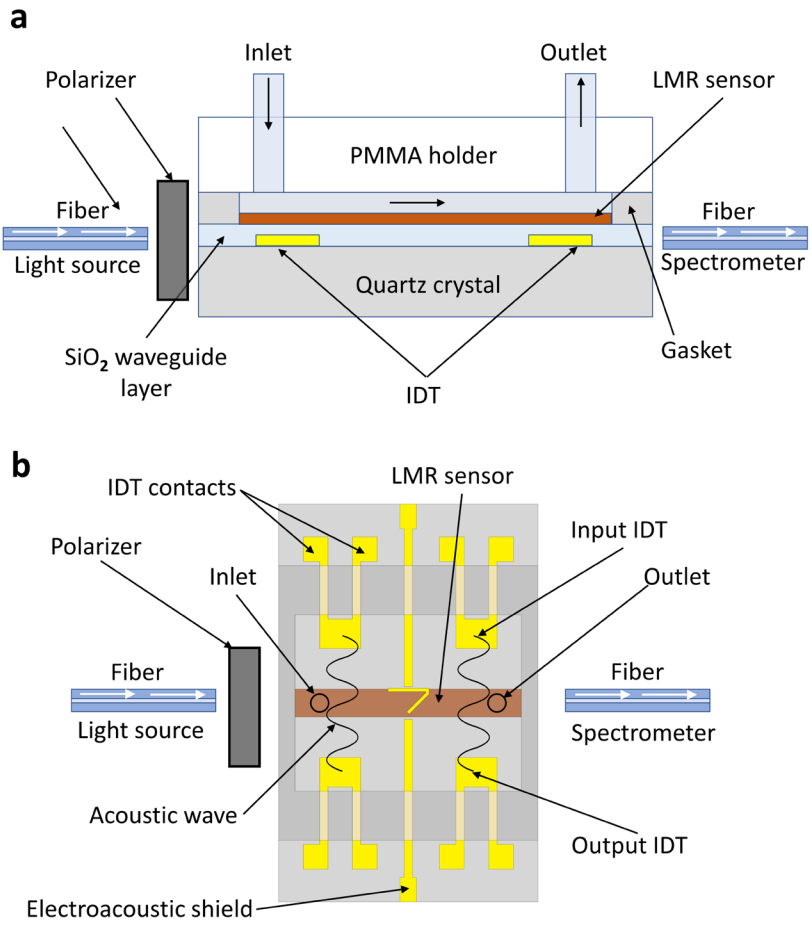

Figure 1: The proposed LMR-SAW platform: ***a.*** *Lateral view with optical propagation path along the LMR sensor* ***b.*** *Top view with dual acoustic propagation path*

2.1. Love-wave sensor

The SAW sensor is based on a piezoelectric delay line with a transmitter and a receiver in the form of interdigital transducers (IDTs), which generates and propagates an acoustic wave [20,21]. This delay line is based on a quartz substrate, AT cut, with interdigitated electrodes composed of 44 split-finger pairs of titanium and gold, in Ti-Au-Ti configuration, 150 nm thick, with a wavelength λ or spatial periodicity 40 μm. The aperture (W) and the acoustic propagation path (IDTs center to center distance Lcc) are equal to 40λ and 210λ respectively. The two long narrow yellow patterns between the two pairs of SAW IDT are electrically grounded, they are used as a shield to better separate electro-acoustically both SAW delay-lines.

The orientation of the IDTs with metal strips perpendicular to the X crystallographic axis allows the generation of pure shear horizontal waves (SH), that do not suffer from excessive loss of acoustic energy with an adjacent liquid medium. A SiO2 overlayer of 3.6 μm is deposited by plasma-enhanced chemical vapor deposition to trap the SH acoustic energy, leading to guided shear horizontal surface acoustic waves, or "Love waves". This confinement of the wave energy near the surface maximizes the sensitivity of the sensor. The contacts have been thickened with gold to improve reliability. These metallic layers have been evaporated using the lift-off process. More details on microfabrication process of this sensor are reported in previous works about graphene oxide Love wave sensor for detection of humidity and VOCs[22].

The generation of LMRs in planar configuration has been demonstrated in some previous works[18,19]. Some of the advantages include the ease of manipulating these sensors, as well as the robustness and ease of encapsulating the surface with microfluidic devices. Also, an advantage is that the SAW sensor has a SiO_2 guiding layer that can be used for light transmission. By deposition of a thickness controlled SnO_2 thin film on the SiO_2 layer, it will be possible to generate one or several LMRs in the optical spectrum. In this way, both SAW and LMR sensors are integrated in the same platform.

2.2. SnO_2 Lossy mode resonance characterization

To generate the optical resonance, a section of the upper face of the SAW sensor was coated with SnO_2 using a K675XD direct current sputtering machine from Quorum Technologies, Ltd., Lewes, UK. For the deposition, an intensity of 120 mA and an argon partial pressure of 1.3×10^{-2} mbar were used. The SnO_2 target, 57 mm in diameter and 3 mm thick, was purchased from Loyal Target Technology Co, Beijing, China. The LW-SAW sensor was placed at a distance of 10 cm from the target. For reasons of strategic design, a small area was deposited with the help of a tape mask. The dimensions of the optical sensor are 1.7 mm × 13.8 mm. The deposited thin-film allows to optically monitor two resonances in transverse magnetic mode. For better understanding, they will be called Lossy-mode resonance 1 (LMR1) and Lossy-mode resonance 2 (LMR2).

2.3. Experimental setup and instruments

The proposed setup platform was designed and built taking into account a large number of aspects, seeking the greatest possible robustness, functionality and ease of use in terms of light transmission, good electrical contact and microfluidics. In Figure 2a, a detailed setup is shown. A TAKHI-HP light source from Pyroistech was used for resonance excitation and the Ocean Optics USB4000 spectrometer for monitoring the transmission spectrum. The use of a linear polarizer LPVIS050 from Thorlabs allows separating the LMR_{TE} or LMR_{TM} respectively and make the resonances deeper and easier to track. Both multimode optical fibers FT200EMT with 200/225 µm core/cladding diameter are from Thorlabs.

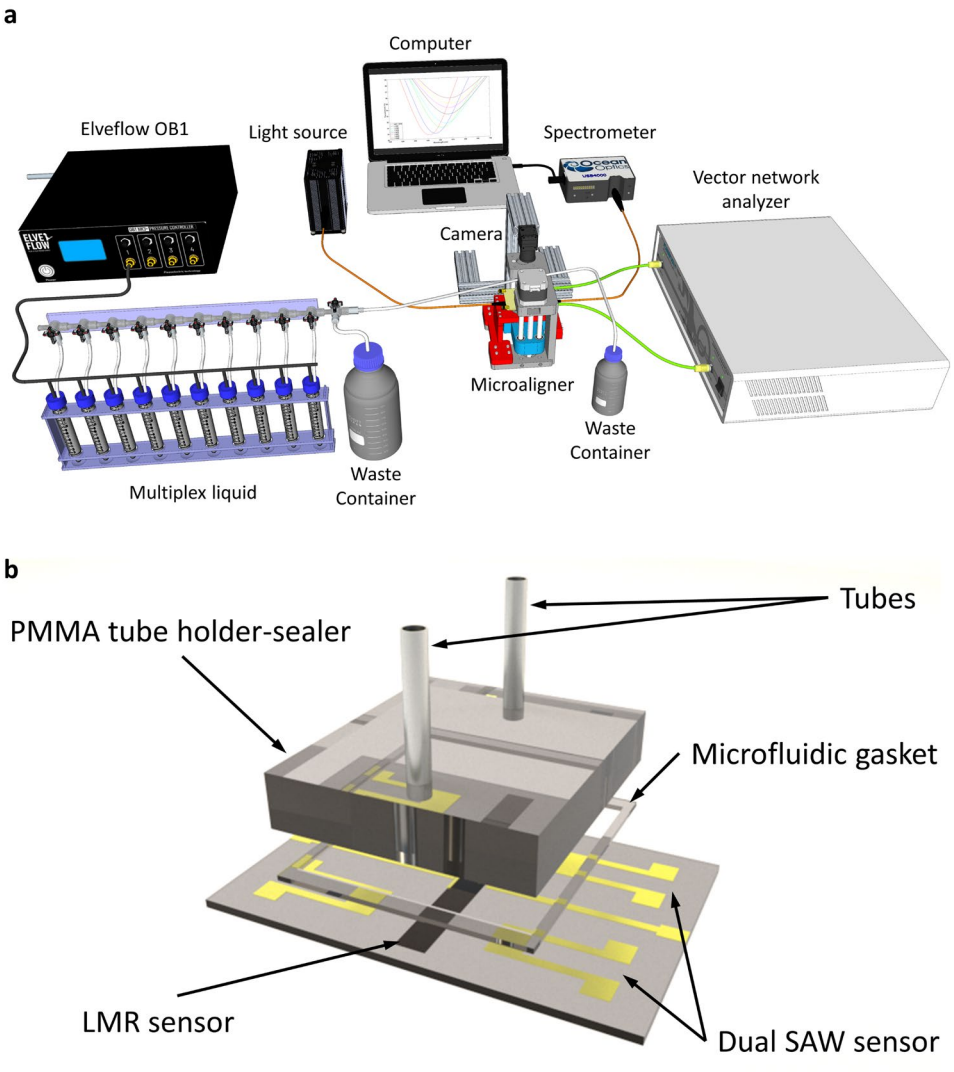

Figure 2: ***a.*** *Experimental setup.* ***b****. Microfluidic gasket with IDTs inside chamber.*

For the generation and acquisition of the acoustic signal, the Planar 304/1 Vector Network Analyzer (VNA) from Copper Mountain Technologies (two-port model) was used. All measurements were obtained at 10 samples/s with a resolution of 10000 points.

To achieve a stable pressure during the experiment, the Elveflow OB1 pressure flow controller was used. The pressure used was 60 mbar. It is also important to visualize the state of the sensor surface at all time, since the accidental introduction of bubbles in the chamber may induce signal distortion in both sensors' response. For this purpose, a high-definition camera USB3 Vision Qf ximea was used to visualize the sensor.

2.4 Basic conditions for the experiments

The experiment was carried out with glucose in water solutions, previously prepared and measured with a refractometer (30GS from Mettler Toledo Inc.). The experiment was performed at room temperature, around 20 ºC. No extra temperature control was used in the setup. The process starts by purging the air from the tubes of each liquid under study. A constant pressure of 60 mbar is used and 3 ml of liquid is displaced in each purge. For this purpose, a stopcock diverts those liquids to a waste container. After purging, the line is cleaned with 15 ml of water. Everything is done with the tube that goes to the connected sensor. In the experiment 5 ml of each liquid is injected sequentially into the sensor. The first and last liquid to be injected is deionized water. Once each liquid is injected, the flow is stopped and the stable state is sampled for 5 minutes.

3. Results

3.1. Lossy-mode resonance

As a verification of the correct operation of the LMR1, its wavelength shift is tested using deionized water. Figure 3a shows the air-water transverse magnetic mode resonance transition in steady state (no flow) of air and then of water. The recorded sensitivity corresponds to a first-order LMR, generated with a 60-nm SnO_2 layer analyzed by profilometry, which is shown in Figure 3b (the red region indicates the non-deposited part and the green region the top of the deposited thin film)

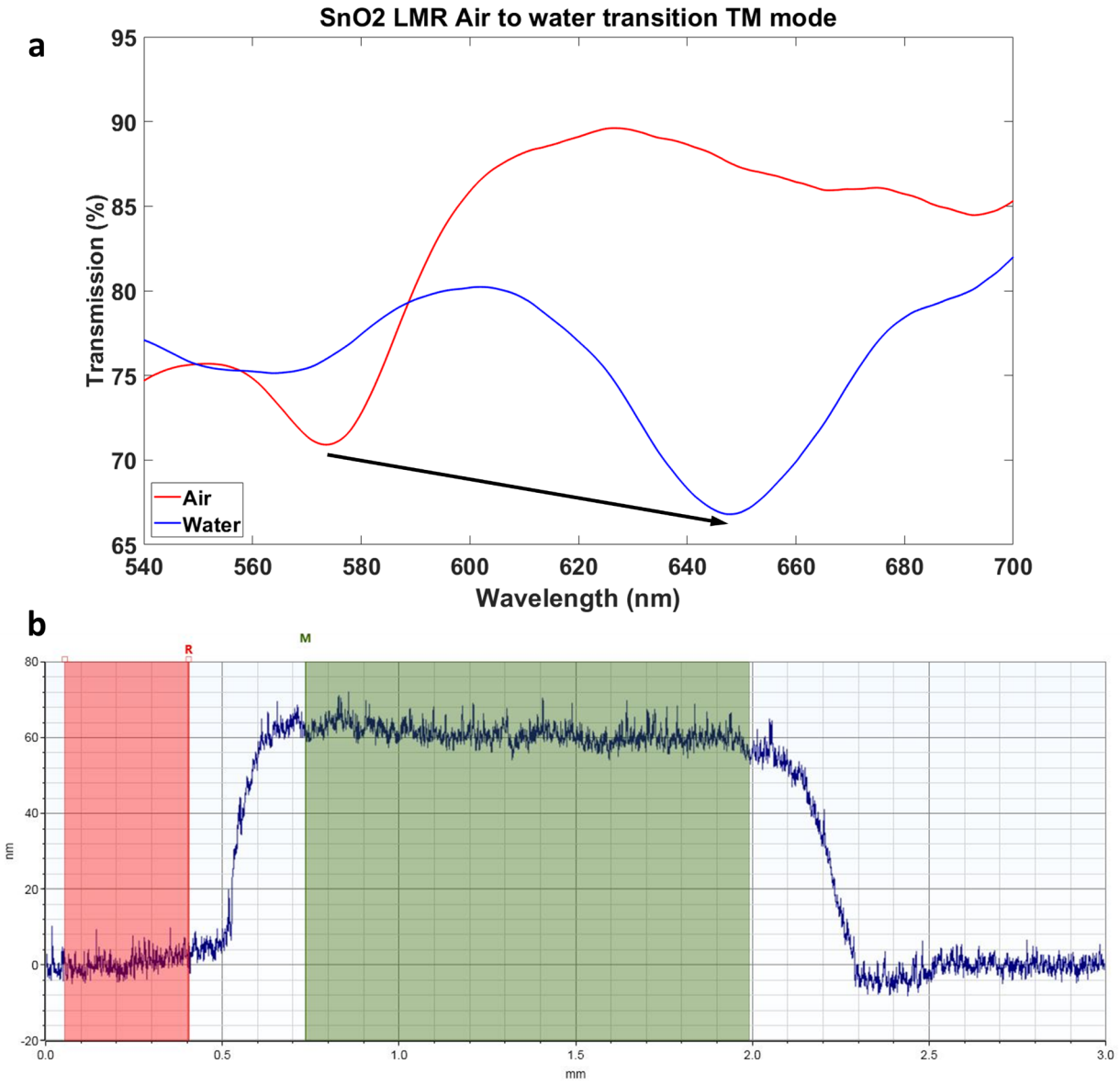

Figure 2: a. Transmission spectrum in air and in water. The LMR resonance experiences a 70 nm wavelength shift. b. Profilometry analysis of the SnO_2 thin film.

3.2. LW-SAW sensor

For comparison, the acoustic insertion losses due the microfluidic system are analyzed with the VNA. Figure 4 shows these insertion losses with and without the microfluidic system on the platform. Evidently there is a reduction of the noise due to the double-glue film, which behaves as an acoustic absorber for outgoing waves. A minimum insertion loss of −30.77 dB

at asynchronous frequency f_0 of about 118.5 MHz is measured. The transmission signal (Scattering parameter S21) of the delay line exposed to the air and then exposed to the water experiences a change in amplitude of almost -10 dB (see ESI† S2). In further LW-SAW signal analysis, the shift of the S11 reflection and S21 transmission parameters are considered (ΔS11 and ΔS21, respectively), with their values in air as reference and taking into account a time-gating post-process in order to focus on the direct acoustic signal, excluding any parasitic ones such as reflections or electrical influence[2].

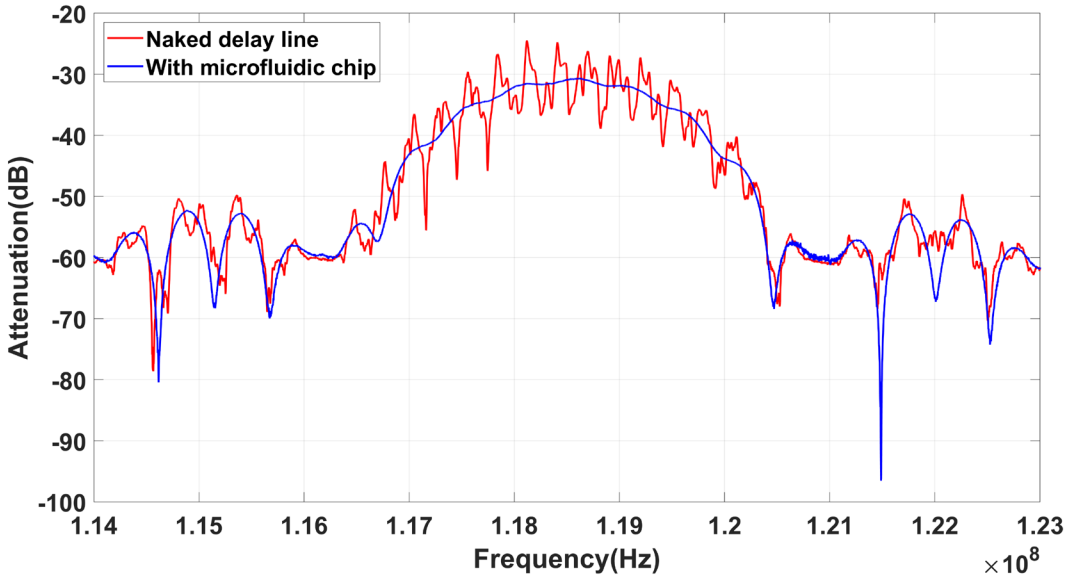

Figure 4: Transmission signal (S21 parameter) of the delay line without and with the microfluidic chip over the sensor.

3.3. LMR-SAW calibration by glucose solution flow

To assess sensor performance, 10 glucose concentrations ranging from 0 (pure deionized water) to 4.99 mol/kg were injected, in 0.555 mol/kg increments. With increasing glucose concentration per volume, there is an increase in the refractive index and viscosity of the test solutions. The solutions used range in refractive index from 1.3318 to 1.4137 and in viscosity from 1.005 mPa·s to 9.0592 mPa·s. The quantities supplied to the sensor ensure a complete filling of the microfluidic chamber, allowing stable values to be measured. Figure 5 shows the course of the experiment where it is observed a good correspondence and synchronism in the acquisition of the optical and acoustic variables. According to the experiment there is a period in which the substances are circulated through the sensor. During this period, the response offered by the sensor is conditioned to the flow of these substances, which is why once the sensor is saturated, the flow stops for 5 minutes. It is during this steady period that the values are taken to calibrate the sensor, thus leaving out any disturbance that the flow rate or any other variable may bring. On average, the LMR has a response time of 1 minute while in the

case of the SAW it takes 2 minutes. These times are conditioned to the speed of the slow flow that has been adopted since the entire surface of the dual sensor must come into contact with the substance under study. Similarly, the comparison of the scattering parameter S11 and the optical resonance LMR1 offers a good synchronous response (see ESI† S3).

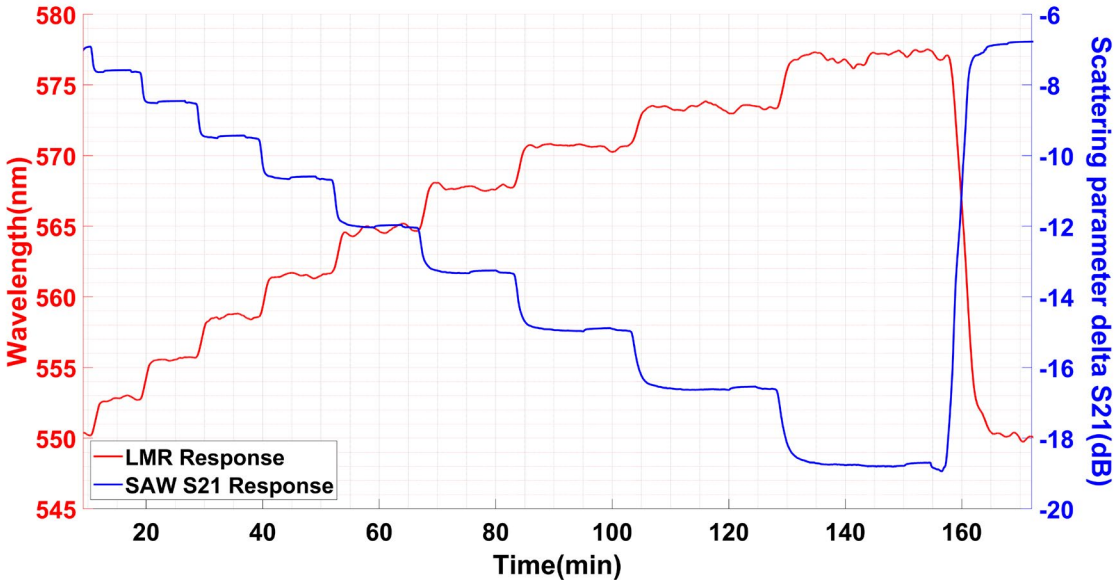

Figure 5: LMR1 wavelength and SAW S21 parameter shift sensorgram.

Also, the sensorgram of the LMR2 resonance with the S21 and S11 parameters of the same experiment offers a synchronous response (see ESI† S4, S5).

3.4. LMR1 calibration

It can be seen in Figure 6a the change in wavelength of the LMR1, corresponding to the different refractive index solutions. A second order polynomial fit has been used. Figure 6b shows the calibration that yields an approximate sensitivity of 332 nm/RIU.

It was possible to monitor the shifts of LMR1 and LMR2 during the experiment (see ESI† S6). Since the spectral shape of the LMR2 resonance undergoes a slight deformation during the shift towards higher refractive indices, it is better to analyze the LMR1, which has a more uniform response.

The detailed spectral evolution of the LMR1 resonance is also obtained and compared to the minimum polynomial second order fit (see ESI† S7). In the same way the non-optimal spectral evolution of LMR2 was obtained (see ESI† S8).

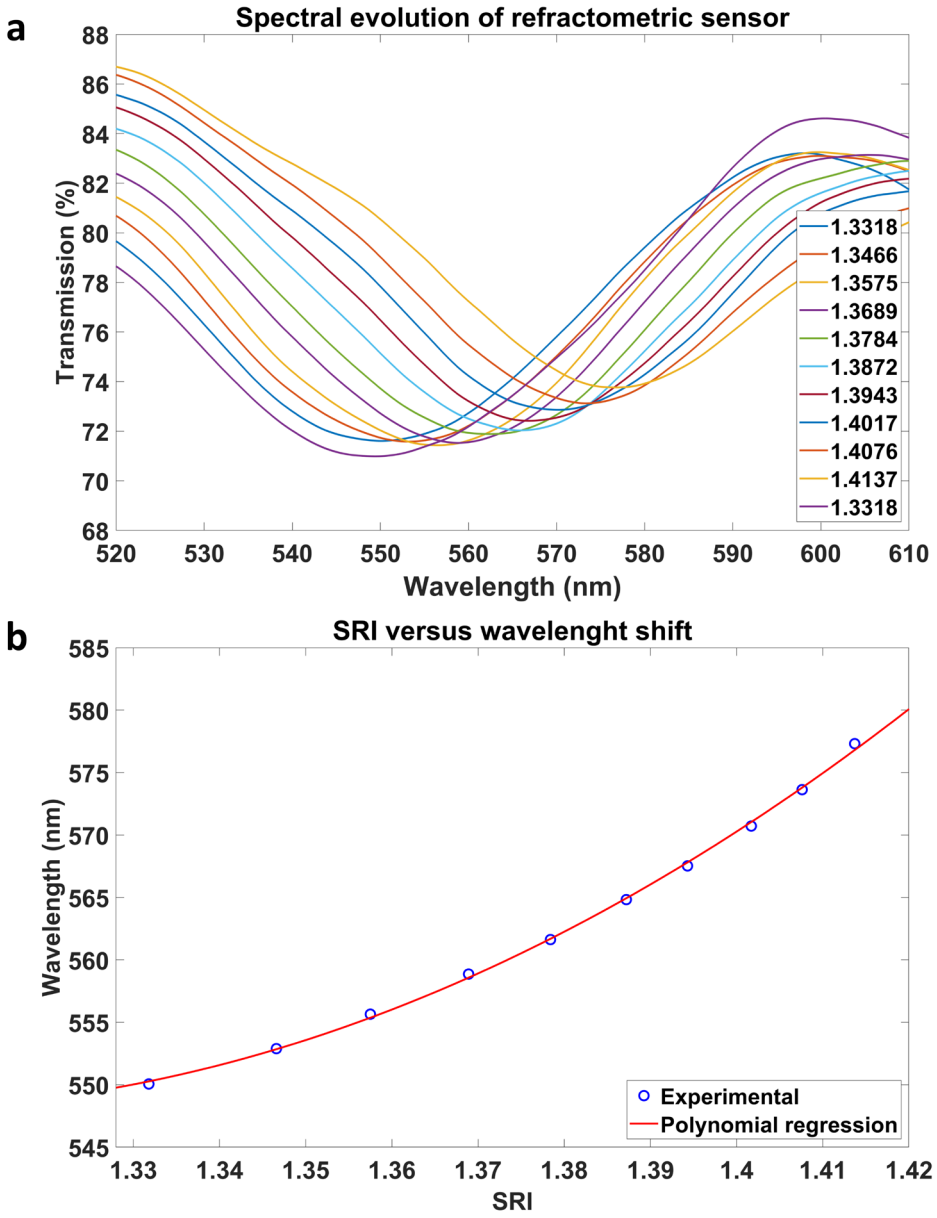

Figure 6: a. Spectral shift of the LMR1 optical resonance obtained during experiment. b. Calibration of the resonance according different SRIs.

3.5. LW-SAW calibration

Similarly, when the surface of the LW-SAW sensor comes into contact with liquid substances, a change in the amplitude and phase of the transmitted acoustic signal is experienced.

The effect of increasing the viscosity and density of the test substance is directly related to the attenuation that occurs in the transmitted signal. Using glucose concentrations is ideal for performing a calibration. Figure 7a shows the evolution of S21 and S11 parameters corresponding to the experiment.

Based on glucose concentrations and using a viscosity model[23], predictive viscosities were calculated for S21, since it is the signal transmitted by the surface of the sensor that is in contact with the substance under study, in addition to the fact that it coincides in the same area with the optical resonance LMR. It can be seen that Figure 7b shows a second order polynomial adjustment of the sensitivity in the range of viscosity explored with a value of -1.5 dB/(mPa·s).

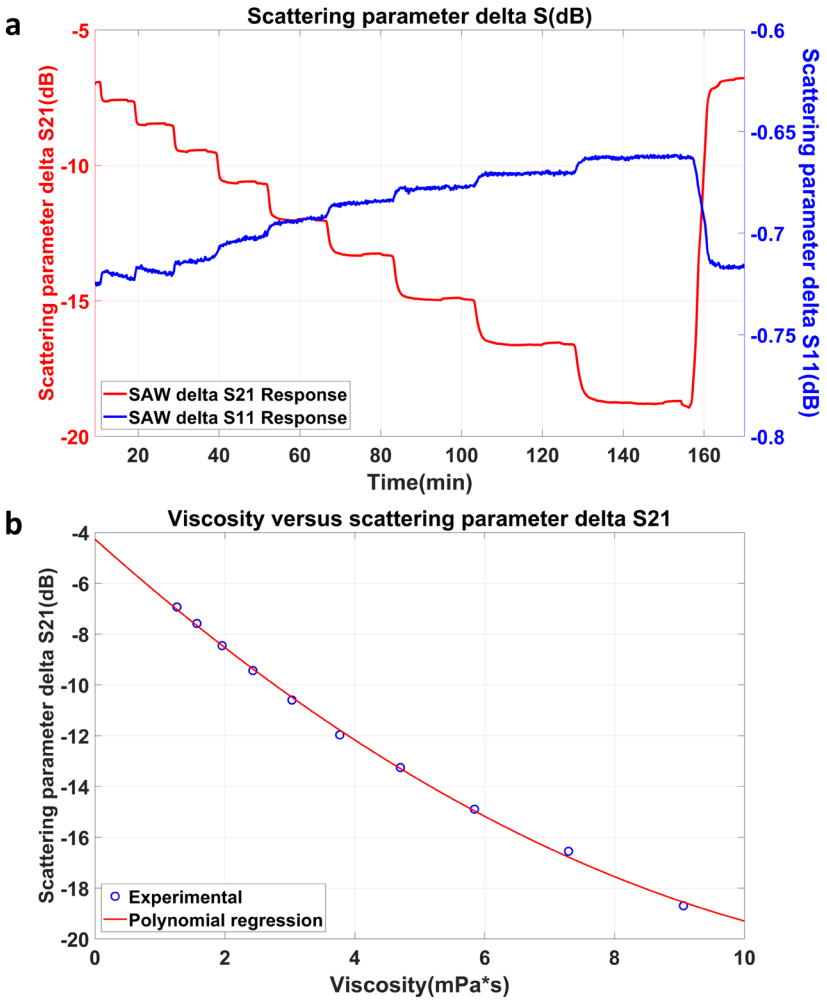

Figure 7 a. Evolution of the ΔS11 and ΔS21 parameters of the LW-SAW sensor. b. Viscosity analysis versus ΔS21 parameter of the SAW device.

4. Conclusions

A new platform for opto-acoustic analysis has been achieved. The combination of classical detection techniques, such as lossy mode resonance (LMR) and surface acoustic wave (SAW) sensors, has been used to simultaneously measure multiple parameters of the same analyte. In the proposed sensing platform, refractive index and viscosity of glucose solutions can be measured in real time requiring a very small volume of analyte for characterization, in the order of microliters. As a result, this method permits to obtain a better knowledge on the properties of a liquid than with techniques where refractive index and viscosity are analyzed separately, with the advantage in terms of saving resources, as a single liquid sample allows for both parameters extraction. Similarly, by having a multiparameter reading, an ambiguous interpretation of the behavior of any of the parameters that influence the measurement can be ruled out.

The proposed sensor has been calibrated experimentally for a refractive index ranging between 1.33 and 1.41, reaching a sensitivity of 332 nm/RIU corresponding to a first order LMR, which is the most sensitive resonance. Viscosity has been successfully tested in ranges from 1.005 mPa·s to 9 mPa·s, demonstrating a sensitivity of -1.5 dB/(mPa·s).

In future designs it will be possible to improve the sensitivity of the sensor. Confining the IDTs outside the microfluidic channel could provide a better SAW sensor response for enhanced mechanical sensing resolution. Besides, keeping IDTs inside the microfluidic channel could provide additional information related to the electrical behavior of the solution. In the same way, it will be interesting to investigate other materials capable of generating LMRs, or even test alternative materials for the waveguide of the SAW sensor like low refractive index polymers.

Finally, this refractometer-viscometer platform could be used for more demanding applications, such as dual characterization of substrate surfaces for molecule binding and label-free biosensing applications. Also, in other fields not linked to life research, there is interest in simultaneously detecting refractive index and viscosity, such as in the case of a possible application in the simultaneous characterization of lubricating oils or transformer insulation and cooling oils[24], given that it is It has been proven that their physical properties change over time due to wear.

Acknowledgments

The authors would like to acknowledge the partial support to the Spanish Ministry of Economy and Competitiveness PID2019-106070RB-I00 and PID2019-106231RB-I00 research funds and the pre-doctoral research grant of the Public University of Navarra. The authors also want to warmly thank Bernard Bobby Ngoune, PhD student at IMS Bordeaux, for valuable help especially in acoustic data acquisition and processing tool (VNA, Python code), as well as Maxence Rubé, University of French Guiana, who has played a major role in the development of the data processing tool during his over 2 years PhD period at IMS Bordeaux.

References

1 J. J. A. Lozeman, P. Führer, W. Olthuis and M. Odijk, Spectroelectrochemistry, the future of visualizing electrode processes by hyphenating electrochemistry with spectroscopic techniques, Analyst, 2020, 145, 2482–2509, DOI: 10.1039/c9an02105a.

2 M. Rube, M. Sebeloue, I. Sadli, L. Linguet, D. Rebiere and C. Dejous, Unconventional protocol for SAW sensor: multi-physic response enrichment in liquid medium, IEEE Sensors Journal, 2021, 22, 12, 11345-11354, DOI: 10.1109/JSEN.2021.3094299.

3 A. G. Samarentsis, A. K. Pantazis, A. Tsortos, J. M. Friedt and E. Gizeli, Hybrid Sensor Device for Simultaneous Surface Plasmon Resonance and Surface Acoustic Wave Measurements, Sensors (Switzerland), 2020, 20, 1–22, DOI: 10.3390/s20216177.

4 F. Bender, P. Roach, A. Tsortos, G. Papadakis, M. I. Newton, G. McHale and E. Gizeli, Development of a combined surface plasmon resonance/surface acoustic wave device for the characterization of biomolecules, Measurement Science and Technology, 2009, 20, 12, DOI: 10.1088/0957-0233/20/12/124011.

5 J. M. Friedt and L. A. Francis, Combined surface acoustic wave and surface plasmon resonance measurement of collagen and fibrinogen layer physical properties, Sens Biosensing Res, 2016, 11, 60–70, DOI: 10.1016/j.sbsr.2016.05.007.

6 C. Campbell, Surface Acoustic Wave Devices for Mobile and Wireless Communications (1st. ed.), Academic Press, Inc., USA, 1998.

7 D. S. Ballantine, Acoustic wave sensors: theory, design, and physico-chemical applications (1st. ed.), AP, 1997.

8 B. Jakoby and M. J. Vellekoop, Properties of Love waves: applications in sensors, Smart Materials and Structures, 1997, 6, 668–679, DOI: 10.1088/0964-1726/6/6/003.

9 I. del Villar, C. R. Zamarreño, M. Hernaez, F. J. Arregui and I. R. Matias, Lossy Mode Resonance Generation with Indium-Tin-Oxide-Coated Optical Fibers for Sensing Applications, Journal of Lightwave Technology, 2010, 28, 111–117, DOI: 10.1109/JLT.2009.2036580.

10 F. Yang and J. R. Sambles, Determination of the optical permittivity and thickness of absorbing films using long range modes, Journal of Modern Optics, 1997, 44, 1155–1163, DOI: 10.1080/09500349708230726.

11 I. del Villar, C. R. Zamarreño, M. Hernaez, F. J. Arregui, I. R. Matias, Z. Y. Wang, J. R. Heflin, R. H. Stolen and S. Ramachandran, Resonances in coated long period fiber gratings and cladding removed multimode optical fibers: a comparative study, OPTICS EXPRESS, 2010, 18, 19, DOI: 10.1364/OE.18.020183.

12 I. Dominguez, I. del Villar, O. Fuentes, J. M. Corres and I. R. Matias, Dually nanocoated planar waveguides towards multi-parameter sensing, Scientific Reports, 2021, 11, 3669, DOI:10.1038/s41598-021-83324-8.

13 I. del Villar, F. J. Arregui, C. R. Zamarreño, J. M. Corres, C. Bariain, J. Goicoechea, C. Elosua, M. Hernaez, P. J. Rivero, A. B. Socorro, A. Urrutia, P. Sanchez, P. Zubiate, D. Lopez, N. de Acha, J. Ascorbe and I. R. Matias, Optical sensors based on lossy-mode resonances, Sensors and Actuators B: Chemical, 2017, 240, 174–185, DOI: 10.1016/j.snb.2016.08.126.

14 S. P. Usha, S. K. Mishra and B. D. Gupta, Fiber optic hydrogen sulfide gas sensors utilizing ZnO thin film/ZnO nanoparticles: A comparison of surface plasmon resonance and lossy mode resonance, Sensors and Actuators, B: Chemical, 2015, 218, 196–204, DOI: 10.1016/j.snb.2015.04.108.

15 F. J. Arregui, I. del Villar, C. R. Zamarreño, P. Zubiate and I. R. Matias, Giant sensitivity of optical fiber sensors by means of lossy mode resonance, Sensors and Actuators, B: Chemical, 2016, 232, 660–665, DOI: 10.1016/j.snb.2016.04.015.

16 F. Chiavaioli, P. Zubiate, I. del Villar, C. R. ZamarrenÌo, A. Giannetti, S. Tombelli, C. Trono, F. J. Arregui, I. R. Matias and F. Baldini, Femtomolar Detection by Nanocoated Fiber Label-Free Biosensors, ACS Sensors, 2018, 3, 936–943, DOI: 10.1021/acssensors.7b00918.

17 P. Zubiate, A. Urrutia, C. R. Zamarreño, J. Egea-Urra, J. Fernández-Irigoyen, A. Giannetti, F. Baldini, S. Díaz, I. R. Matias, F. J. Arregui, E. Santamaría, F. Chiavaioli and I. del Villar, Fiber-based early diagnosis of venous thromboembolic disease by label-free D-dimer detection, Biosensors and Bioelectronics: X, 2019, 2, DOI: 10.1016/j.biosx.2019.100026.

18 O. Fuentes, I. del Villar, J. M. Corres and I. R. Matias, Lossy mode resonance sensors based on lateral light incidence in nanocoated planar waveguides, Scientific Reports, 2019, 9, 8882, DOI:10.1038/s41598-019-45285-x.

19 I. Dominguez, J. M. Corres, O. Fuentes, I. del Villar and I. R. Matias, Multichannel Refractometer based on Lossy Mode Resonances, IEEE Sensors Journal, 2022, 22, 3181–3187, DOI 10.1109/JSEN.2022.3142050.

20 V. Raimbault, D. Rebière, C. Dejous, M. Guirardel and V. Conedera, Acoustic Love wave platform with PDMS microfluidic chip, Sensors and Actuators, A: Physical, 2008, 142, 160–165, DOI: 10.1016/j.sna.2007.05.026.

21 C. Dejous, H. Hallil, V. Raimbault, J. L. Lachaud, B. Plano, R. Delépée, P. Favetta, L. Agrofoglio and D. Rebière, Love AcousticWave-Based Devices and Molecularly-Imprinted Polymers as Versatile Sensors for Electronic Nose or Tongue for Cancer Monitoring, Sensors (Switzerland), 2016, 16, 915, DOI:10.3390/s16060915.

22 I. Nikolaou, H. Hallil, B. Plano, G. Deligeorgis, V. Conedera, H. Garcia, C. Dejous and D. Rebière, Drop-casted Graphene Oxide Love Wave sensor for detection of humidity and VOCs, Journal of Integrated Circuits and Systems, 2016, 11, 49–56, DOI: 10.29292/jics.v11i1.429.

23 A. Viet Bui and M. H. Nguyen, Prediction of viscosity of glucose and calcium chloride solutions, Journal of Food Engineering, 2004, 62, 345–349, DOI: 10.1016/S0260-8774(03)00249-8.

24 Prasintha, Pamelia & Sari, Dyah & Ridho, Rosit & Fikroh, Uliz & Unair, Pujiyanto & Trilaksana, Herri & Samian, Samian. (2020). Detection of lubricating oil viscosity based on displacement sensor using fiber coupler and concave mirror. AIP Conference Proceedings. 2314. 030010. DOI: 10.1063/5.0034554.